Cascade system using both trough system and dish system for power generation

1 Introduction

Energy is the crucial part for the infrastructure and maintenance of society. With the increase amount of energy consumption, our quality of life has been improved significantly. However, nowadays the world energy consumption is highly dependent on fossil fuels, which supplied 81.3% of the world's energy consumption in 2012 according to the data of World Bank Group. Using fossil fuels a lot is afflicting the environment, which is sacrificing our quality of life. Environmental pollutions and global warming are becoming serious problem, and it is urgent to find clean and renewable energy to substitute the fossil fuels.

Solar energy is a clean, sustainable, wide-distributed energy. The total amount of solar energy is very huge. The amount of sunlight striking the earth's atmosphere continuously is 1.75×10^5 TW, even if 1% of it could be converted into electric energy with a 10% efficiency, it would produce 175 TW, much larger than the total global energy needs predicted to be 25-30 TW in 2050 [1]. But at the same time, solar energy has some disadvantages for its low flux density and large fluctuation due to daily and seasonal variations exacerbated by variations owing to weather. Concentrated solar power (CSP) technology has the ability to overcome these disadvantages and believed to be the future power generation technology.

There are 4 common forms of CSP technologies, parabolic trough, dish Stirlings, concentrating linear Fresnel receiver, and solar power tower. Different types of collectors and different technologies for electricity generation are suitable for different working temperature zones with different costs. Combination of different collectors with different technologies may provide a new direction to achieve higher efficiency with lower cost for CSP.

Cau [2] reported a comparative performance analysis of CSP plants using parabolic trough and linear Fresnel collectors, thermal oil as heat transfer fluid and an Organic Rankine Cycle (ORC) power generation unit. A two-tank direct thermal storage system are included and in the Rankine cycle, regenerator, 4 6 steam extractions and air-cooler condenser are used. The performance analysis of the two types of system shows that CSP plants based on linear Fresnel collectors lead to higher values of electrical energy production per unit area of land and CSP plants based on parabolic troughs gives better values of energy production per unit area of collector.

Franchini [3] carried out simulations to predict the performance of a Solar Rankine Cycle (SRC) and an Integrated Solar Combined Cycle (ISCC) when combined with two different solar field configurations based on parabolic trough collectors (PTCs) and power tower (PT) systems. The comparative analysis was mainly focused on the influence of CSP technology on global solar energy conversion efficiency of both SRC and ISCC plants. Results show that both higher collection efficiency and conversion efficiency of ST compared to PTCs in both SRC and ISCC situations.

Cipollone [4] discussed some thermodynamic and engineering aspects concerning the use of parabolic troughs for heating gasses of gas turbines. They further discussed the Discrete Ericsson Cycle (DEC), in the cycle, a sequence of

intercooled compressions and reheated expansions is deployed to increase cycle specific work and efficiency. They applied optimization adopting as design parameter the power per unit of collector length, and pointed out that the number of compressions and expansions could not exceed three stages.

Behar [5] reviewed the R&D activities and published studies on integrated solar combined cycle system (ISCCS), various configurations have been proposed with their performance investigated. The paper also introduced lots of software or mathematical programs to simulate the performance of various design.

Ghaem [6] investigated and compared the performance of various configurations of hybrid solar dish-Brayton cycle. A thermodynamic model implemented in Engineering Equation Solver (EES) is developed for various configurations. Results show that the model in which receiver located before the turbine can achieve higher performance compare to the one in which the receiver located after the turbine. Simulation of the models pointed out that a comprehensive well defined control algorithm is a vital issue in order to control engine operation, solar input heat flux and sun tracking system.

In this paper, an idea of cascade collection and cascade utilisation of solar energy with higher efficiency is presented. Parabolic trough collectors are used to collect lower temperature energy with lower cost and dish collectors are used to collect higher temperature energy with higher efficiency. Rankine cycle is used to work in lower temperature zone and Stirling cycle is used to work in higher temperature zone. Furthermore, effective topological structures are considered to take full advantages of thermodynamic characters of different components of the system. The cold chamber of Stirling engine is cooled by condensed fluid of Rankine cycle to use the heat released by Stirling engine.

First, the idea of cascade system is presented and the feasibility analysis of the system is performed. A conceptual sketch of the system is presented with some important state points. Second, based on this sketch, some components are chosen and some key parameters of the system are given. Third, models of components are built according to their thermodynamic properties. Models of different circuits are built with these component models and efficiency can be obtained by the circuit data. Fourth, two separate systems, dish-Stirling system and trough-Rankine system, are built for comparison. At last, the models of the systems are calculated and results are analysed.

2 System description and specification

In the cascade system, dish collectors are used to provide heat for Stirling engines and air-to-water heat exchanger. Trough collectors are used to provide heat for preheating, evaporating and superheating in the Rankine cycle. Figure 1 shows the sketch of the cascade system. Water is used as the working fluid of Rankine cycle, which is heated in the cold chamber of Stirling engines, preheater, evaporator, superheater, and air-to-water heat exchanger successively, and then expand in turbine, condense in condenser. Pumps are used to change the pressure of fluids. Stirling engines are used for power generation and cooled

by feed water of the Rankine cycle. State number pairs of different fluids are marked on the sketch. The first number of a number pair indicates the type of the fluid, the second number of a number pair indicates the state point of the fluid. Number pairs with solid circle indicate saturated liquid states ($x = 0$), and with dotted circle indicates saturated gas states ($x = 1$). Figure 2 shows the T-s diagram of the water circuit in the cascade system. In this Rankine cycle, the heat released in process 2,5-2,6 can be utilized by series of Stirling engines, which may increase the power of Rankine cycle. Figure 3 shows the heat transfer diagram of this process.

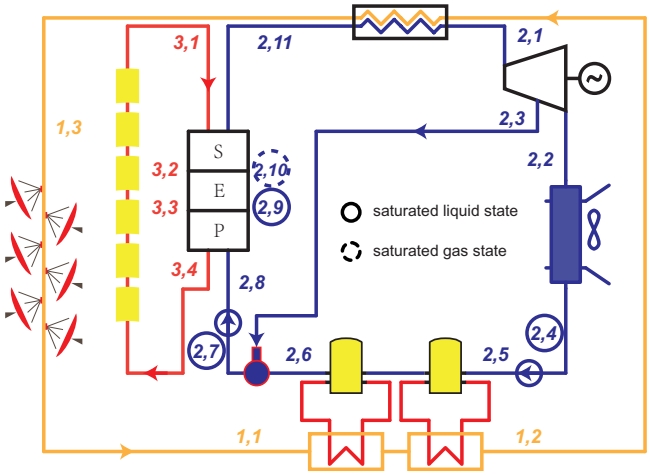

Figure 1: Sketch of the cascade system

To build the cascade system model, several simplifying assumptions are made:

- Steady state at nominal load of the system is analyzed
- Pressure drop due to flow is negligible
- The leak of working fluid in the pipes is neglected
- Same isentropic efficiency of steam turbine with different loads and in different stages
- Heat loss that occurs from the tube to the atmosphere is not considered
- There is no heat loss to the environment for Stirling engines
- Simple models are used of some processes and equipments

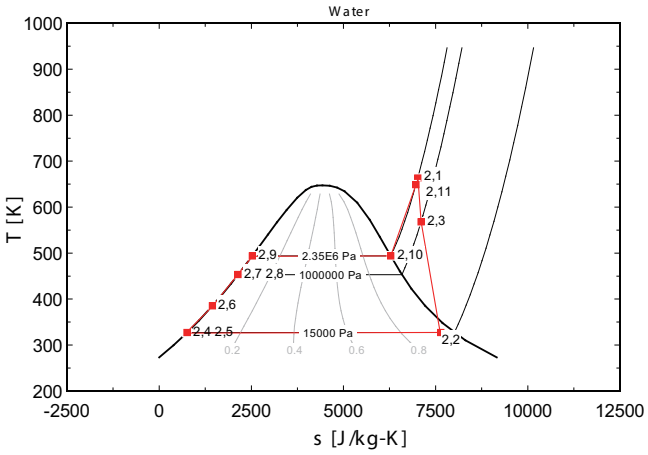

Figure 2: T-s diagram of the water circuit

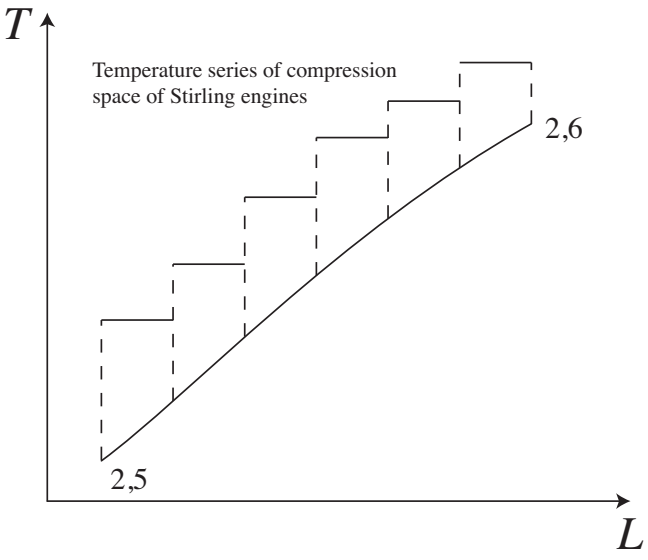

Figure 3: Heat transfer diagram of process 2,5-2,6

- A symmetrical regenerator behaviour is assumed so that a single effectiveness can be defined as $e = \dfrac{T_R - T_L}{T_H - T_L}$ [7, 8]

Table 1 shows the basic design parameters of the cascade system.

Table 1: Basic design parameters of the cascade system

Parameters	Value
I_{DNI}	700 W/m^2
T_{amb}	293 K
p_{amb}	1×10^5 Pa
v_{wind}	4 m/s
$P_{generator}$	6×10^6 W
$T_{dish,inlet}$	623K
$T_{dish,outlet}$	1073 K
p_{dish}	5×10^5 Pa
$\Delta T_{oil,water,min}$	15 K
$T_{trough,outlet}$	623 K
p_{trough}	2×10^6 Pa
$T_{1,afterstirling}$	673 K
$n_{stirlingEngine}$	100
T_s	340°C
p_s	2.35×10^6 Pa
p_c	1.5×10^4 Pa
$T_{s,d}$	390°C
$p_{deaerator}$	1×10^6 Pa

3 System model

An EES model was built to investigate the characteristics of the cascade system. The cascade system is built in several blocks. These blocks are made of circuits with efficiency calculations. Three circuits, air circuit, water circuit and oil circuit, are built with some specific state parameters in some key components. Energy-based models of these key components are created on the basis of their thermodynamic behavior, heat transfer and the second law.

The following parts introduce models of some key components.

3.1 Dish collector

The most complicate part of the dish collector is the dish receiver. In our cascade system, the structure of the dish receiver is as shown in Figure 4. This section mainly describes dish receiver.

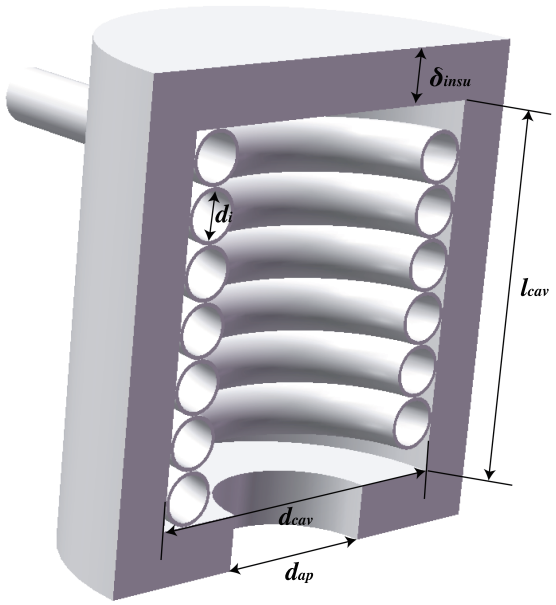

Figure 4: Structure of the dish receiver

Fraser, in his dissertation [9], built a performance prediction model of Stirling dish system with detailed description. The model is also used in the software SAM, which provides performance and financial models for facilitate decision in the renewable energy industry. The dish collector model in the dissertation considers various heat losses, which is a good reference for the dish receiver model of the cascade system.

A dish collector product of SES used in Fraser's dissertation, which is also used in this system, and its parameters are listed in Table 2 [9].

The dish receiver model concerns the losses include: collector losses due to mirror reflectivity, receiver intercept losses, losses due to shading, and thermal losses. Thermal losses take the largest portion of all those losses, which are due to conduction, convection and radiation. Figure 5 shows the heat network of dish receiver, which concerns the losses:

- Radiation losses reflected off of the receiver cavity surfaces and out of the receiver through the aperture. ($q_{rad,reflect}$)
- Conductive losses through the receiver insulating layer. ($q_{cond,tot}$)
- Free convection from the cavity in the absence of wind. ($q_{conv,free}$)

Table 2: Parameters of the dish collector

Parameters	Value
d_{cav}	0.46 m
δ_{insu}	0.075 m
l_{cav}	0.23 m
d_{ap}	0.184 m
λ_{insu}	0.06 W/(m·K)
ϵ_{insu}	0.6
α_{cav}	0.87
δ_a	0.005 m
$d_{i,air}$	0.07 m
A_{dC}	87.7 m^2
θ_{dish}	45°
γ	0.97
$\eta_{shading}$	0.95
ρ	0.91

- Forced convection in the presence of wind. ($q_{conv,forced}$)
- Emission losses due to thermal radiation emitted from the receiver aperture. ($q_{rad,emit}$)

$q_{dish,air}$ can be written as

$$q_{dish,air} = h_{dish,air} A_{dish,air} \Delta T_{ln,Drec,air}$$

where

$$h_{dish,air} = Nu_{tube} \lambda_{dish,air} / d_{i,air}$$

$$Nu_{tube} = c_r Nu'_{tube}$$

For helical spiral pipe, multiplier c_r based on curvature ratio can be written as [10]

$$c_r = 1 + 3.5 \frac{d_{i,air}}{d_{cav} - d_{i,air} - 2\delta_a}$$

Nu'_{tube} is the Nusselt number of straight circular tube, which can be obtained by [11]

$$Nu'_{tube} = 0.027 Re_{tube}^{0.8} Pr_{tube}^{1/3} (\mu_{tube}/\mu_{tube,w})^{0.14}$$

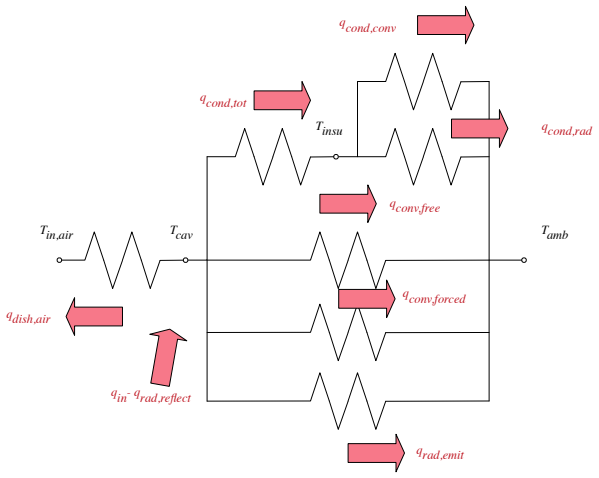

Figure 5: Heat network of dish receiver

$$c_r = 1 + 3.5\frac{d_{i,air}}{d_{cav} - d_{i,air} - 2\delta_a}$$

and $\Delta T_{ln,Drec,air}$ can be written as

$$\Delta T_{ln,Drec,air} = \frac{(T_{cav} - T_{dish,inlet}) - (T_{cav} - T_{dish,outlet})}{\ln \dfrac{T_{cav} - T_{dish,inlet}}{T_{cav} - T_{dish,outlet}}}$$

To get $q_{dish,air}$, T_{cav} is required. As shown in Figure 5, we need to solve the heat network.

$$q_{in} = q_{rad,reflect} + q_{dish,air} + q_{cond,tot} + q_{conv,tot} + q_{rad,emit} \tag{1}$$

q_{in} and η_{dC} can be obtained by

$$q_{in} = I_{DNI} \cdot A_{dC} \gamma \eta_{shading} \rho \tag{2}$$

$$\eta_{dC} = q_{dish,air} / \left(I_{DNI} \cdot A_{dC}\right) \tag{3}$$

Other losses are presented in following sections.

3.1.1 Reflected loss of dish receiver

To determine the reflected loss of the cavity surfaces of the dish receiver $q_{rad,reflect}$, the effective absorptance of the cavity receiver α_{eff} is required to

determine the fraction of energy reflected out of the receiver. The effective absorptance of a cavity receiver without a receiver aperture cover is given by Equation (4) where α_{cav} is the cavity surface absrptance, A_a is the cavity aperture area, and A_{cav} is the total inner surface area of the cavity [12]. Sandra National Laboratories gave an estimate value of the absorptance of the cavity surface α_{cav} of an existing Stirling dish receiver to be 0.87 [13]. To achieve higher effective absorptance, a smaller ratio of the two surface area should be used. But the ratio is constrained by the concentration ratio of the receiver.

$$\alpha_{eff} = \frac{\alpha_{cav}}{\alpha_{cav} + (1 - \alpha_{cav})\,(A_{ap}/A_{cav})} \tag{4}$$

$$q_{rad,reflect} = q_{in}(1 - \alpha_{eff})$$

3.1.2 Conduction loss of dish receiver

Conduction loss of dish receiver $q_{cond,tot}$ equals to the different two parts: convection loss from the insulating layer to the atmosphere $q_{cond,conv}$ and radiation loss from the insulating layer to the atmosphere $q_{cond,rad}$. Both of the two parts are related to the temperature of insulating layer T_{ins}.

$$q_{cond,tot} = \frac{T_{cav} - T_{insu}}{\ln \dfrac{d_{cav} + 2\delta_{insu}}{d_{cav}} / (2\pi\lambda_{insu} l_{cav})}$$

$$\begin{aligned} q_{cond,conv} &= h_{insu} A_{insu} (T_{insu} - T_{amb}) \\ &= \frac{k_{insu} Nu_{insu} A_{insu} (T_{insu} - T_{amb})}{d_{cav} + 2\delta_{insu}} \end{aligned}$$

where Nu_{insu} can be obtained by the correlation for flow over a circular cylinder. [14]

$$q_{cond,rad} = \epsilon_{insu} A_{insu} \sigma (T_{insu}^4 - T_{amb}^4)$$

And

$$q_{cond,tot} = q_{cond,conv} + q_{cond,rad}$$

3.1.3 Convection loss of dish receiver

Ma [15] conducted tests to determine the free convection losses from the receiver for alternative setups, and the data were consistent with Stine and McDonald's free convection correlation. It is assumed that forced convection is independent of free convection in the receiver, so the total convection losses can be represented as the sum of the free and forced convection losses as shown in Figure 5.

$$q_{con,tot} = (h_{free} + h_{forced}) A_{cav} (T_{cav} - T_{amb})$$

where $h_{free} = k_{film} Nu_{free} / \overline{d_{cav}}$, $\overline{d_{cav}} =$.

Wu [16] present a comprehensive review and systematic summarization of convection heat loss from cavity receiver in parabolic dish solar thermal power system. And we choose the correlation presented by Leibfried [17]. This correlation gives an extended model of Koenig [18] and Stine [19] with better results.

For forced convection loss, side-on wind convection loss model given by Ma [15], which is independent of the aperture orientation, is used

$$h_{forced} = 0.1967 v_{wind}^{1.849}$$

3.2 Trough collector

LS-3 is used as the trough collector, its sketch is shown in Figure 6, its parameters are listed in Table 3.

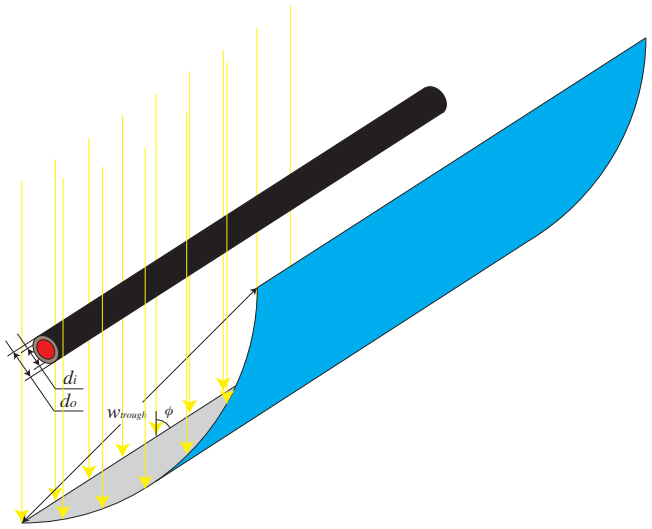

Figure 6: Sketch of trough collector

$$q^{''} = I_{DNI} w_{trough} \eta_{opt,0} K(\phi) F_e / P$$

where $P = \pi d$, $K(\phi)$ is the incidence angle modifier, $\eta_{opt,0}$ is peak optical efficiency (optical efficiency with an incidence angle of 0).

Assume overall heat transfer coefficient $U(T_{abs})$ is uniform for whole length, so that we can use the heat transfer correlation in Appendix **??**.

$$\frac{T_o - T_{amb} - \frac{q^{''}}{U(T_{abs})}}{T_i - T_{amb} - \frac{q^{''}}{U(T_{abs})}} = \exp(-\frac{U(T_{abs})PL}{q_m c_p}) \tag{5}$$

Table 3: Parameters of the trough receiver

Parameters	Value
A_{tC}	545 m^2
w_{trough}	5.76 m
d_i	0.066 m
d_o	0.07 m
ρ	0.94
γ	0.93
τ	0.95
α_{abs}	0.96
F_e	0.97
ϕ	70°

Since the Nu in the pipe is very large (about 1×10^4), small temperature difference exists between the absorber and oil. So $(T_i + T_o)/2$ can be used as the average value of T_{abs}, and $U(T_{abs})$ can be obtained by the a second-order polynomial function given by Romero[20]. Then using Equation (5), we can get the length L required to get the required number of trough collectors in a row.

The efficiency of the trough collector

$$\eta_{trough} = \frac{q_m(h_{out} - h_{in})}{I_{DNI} w_{trough} L}$$

3.3 Stirling engine array

Stirling engine array is used in the cascade system, Figure 7 shows the layout of the Stirling engine array. Each Stirling engine in the Stirling engine array has the identical parameters: $U_{stirling,1} = 30\,\mathrm{W/m^2{\cdot}K}$, $U_{stirling,2} = 150\,\mathrm{W/m^2{\cdot}K}$, $A_{stirling,1} = 6\,\mathrm{m^2}$, $A_{stirling,2} = 6\,\mathrm{m^2}$, $k_{stirling} = 1.4$, $\gamma_{stirling} = 3.375$, $n = 7.84 \times 10^{-2}\,\mathrm{mol}$, $n_{se} = 10\,\mathrm{s^{-1}}$.

Depending on the flow directions of heating and cooling flows, there are two flow types: parallel flow and counter flow. Figure 8 and Figure 9 show the heat transfer diagrams of the two flow types.

In Figure 7, $T_{1,i,1} = T_{1,i}, q_{m,1,r} = q_{m,1}/n_2$. For x from 1 to $n_1 - 1$, where x is the column number of Stirling engine, $T_{1,i,x+1} = T_{1,o,x}, T_{2,i,x+1} = T_{2,o,x}$.

Assume that the positive flow direction is to the right, for parallel flow,

$$T_{2,i,1} = T_{2,i}$$

$$q_{m,2,r} = q_{m,2}/n_2$$

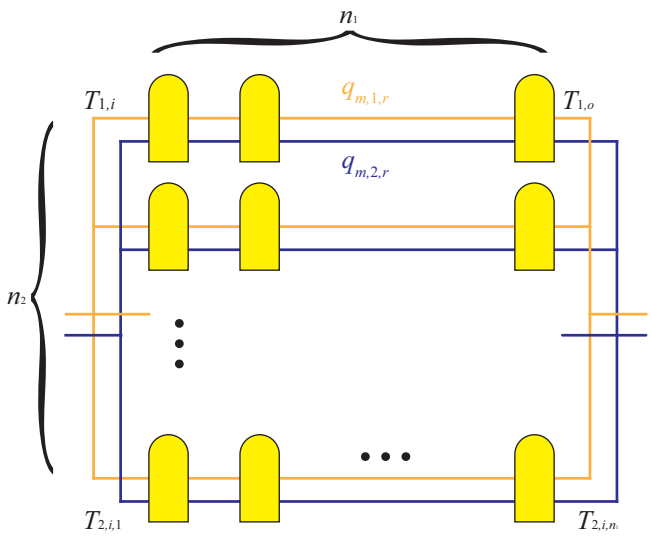

Figure 7: Layout of Stirling engines

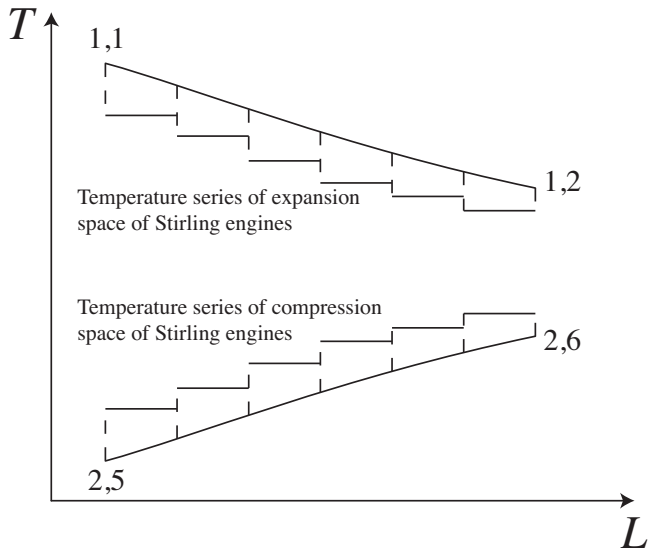

Figure 8: Heat transfer diagram of parallel flow

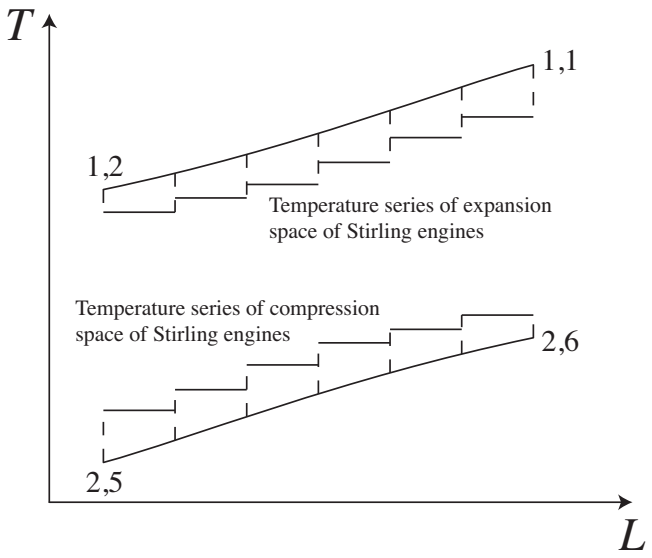

Figure 9: Heat transfer diagram of Counter flow

for counter flow,

$$T_{2,o,n_1} = T_{2,i}$$
$$q_{m,2,r} = -q_{m,2}/n_2$$

For a Stirling engine in column x, x from 1 to n_1, according to Appendix,

$$T_{H,x} = T_{1,i,x} - \frac{T_{1,i,x} - T_{1,o,x}}{1 - \exp(-\frac{U_{stirling,1} A_{stirling,1}}{q_{m,1,r} c_{p,1,x}})}$$
$$T_{L,x} = T_{2,i,x} - \frac{T_{2,i,x} - T_{2,o,x}}{1 - \exp(-\frac{U_{stirling,2} A_{stirling,2}}{q_{m,2,r} c_{p,2,x}})}$$

Assuming a linear temperature profile across the regenerator, the mean effective temperature $T_{R,x} = \frac{T_{H,x} - T_{L,x}}{\ln(T_{H,x}/T_{L,x})}$ [21, 22], and the symmetrical regenerator behaviour assumption $e_x = \frac{T_{R,x} - T_{L,x}}{T_{H,x} - T_{L,x}}$ [7, 8], then the efficiency of Stirling engine in column x can be written as [23, 1]

$$\eta_{stirling,x} = \frac{T_{H,x} - T_{L,x}}{T_{H,x} + \frac{1 - e_x}{k - 1} \cdot \frac{T_{H,x} - T_{L,x}}{\ln \gamma_{stirling}}}$$

For energy balance,

$$q_{m,1,r}(h_{1,i,x} - h_{1,o,x})(1 - \eta_{stirling,x}) = q_{m,2,r}(h_{2,o,x} - h_{2,i,x})$$

And in each Stirling cycle, the heat absorbed by the working gas is

$$nR\left(T_{H,x}\ln\gamma_{stirling} + \frac{1-e_x}{k-1}\left(T_{H,x} - T_{L,x}\right)\right) = q_{m,1,r}(h_{1,i,x} - h_{1,o,x})/n_{se}$$

By solving above equations, efficiency of the Stirling engine array $\eta_{stirling}$ can be obtained by

$$\eta_{stirling} = 1 - \frac{q_{m,2}(h_{2,o,n_1} - h_{2,i,1})}{q_{m,1}(h_{1,i,1} - h_{1,o,n_1})}$$

and power of Stirling engine in column x

$$P_{stirlingEngine,x} = q_{m,1,r}(h_{1,i,x} - h_{1,o,x})\eta_{stirling,x}$$

and power of the Stirling engine array

$$P_{stirling} = \eta_{stirling}q_{m,1}(h_{1,i,1} - h_{1,o,n_1})$$

3.4 Steam turbine

A steam turbine product, N-6 2.35, of Qingdao Jieneng Power Station Engineering Co., Ltd is used for calculation. Its isentropic efficiency $\eta_{i,turbine}$ can be obtained by the given design parameters.

Using basic design parameters in Table 1, parameters of state 2,2 and 2,3 in Figure 1 of the steam turbine can be obtained by the following equations.

$$\eta_{i,turbine} = \frac{h_{2,1} - h_{2,2}}{h_{2,1} - h_{i,2,2}}$$

$$\eta_{i,turbine} = \frac{h_{2,1} - h_{2,3}}{h_{2,1} - h_{i,2,3}}$$

The output power of steam turbine

$$P_{turbine} = (1-y)\,q_{m,2}\,(h_{2,1} - h_{2,2}) + yq_{m,2}\,(h_{2,1} - h_{2,3})$$

The sum power of pumps

$$P_{pump} = (1-y)\,q_{m,2}\,(h_{2,5} - h_{2,4}) + q_{m,2}\,(h_{2,8} - h_{2,7})$$

Heat injected in the water circuit

$$Q_2 = (1-y)\,q_{m,2}\,(h_{2,6} - h_{2,5}) + q_{m,2}\,(h_{2,1} - h_{2,8})$$

The efficiency of Rankine cycle can be expressed as

$$\eta_{rankine} = (P_{turbine} - P_{pump}/\eta_{generator})/Q_2$$

4 Separate system models

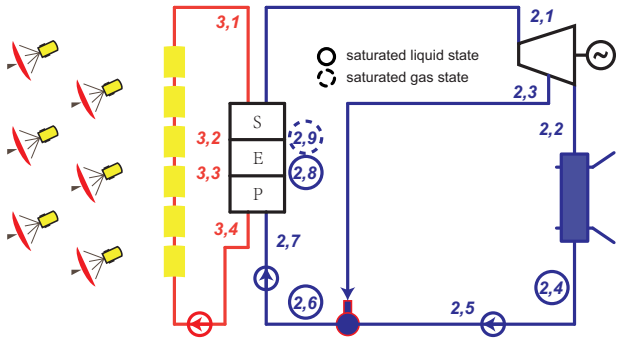

Figure 10: Sketch of the separate systems

Figure 10 shows the sketch of the separate systems. These two separate systems are built for comparison. They use the same dish collectors and trough collectors. They have the same thermal efficiencies.

4.1 Separate trough system

Steam turbine has the same main parameters and same isentropic efficiency with that of the cascade system. Pressure of deaerator are the same of the cascade system. So parameters of state 2,2 and 2,3 in Figure 10 of the steam turbine can be obtained by the following equations.

$$\eta_{i,turbine} = \frac{h_{2,1,s} - h_{2,2,s}}{h_{2,1,s} - h_{i,2,2,s}}$$

$$\eta_{i,turbine} = \frac{h_{2,1,s} - h_{2,3,s}}{h_{2,1,s} - h_{i,2,3,s}}$$

The output power of steam turbine

$$P_{turbine,s} = (1 - y_s)\, q_{m,2,s}\, (h_{2,1,s} - h_{2,2,s}) + y_s q_{m,2,s}\, (h_{2,1,s} - h_{2,3,s})$$

The output power of generator

$$P_{generator,s} = P_{turbine,s} \eta_{generator}$$

The sum power of pumps

$$P_{pump,s} = (1 - y_s)\, q_{m,2,s}\, (h_{2,5,s} - h_{2,4,s}) + q_{m,2,s}\, (h_{2,7,s} - h_{2,6,s})$$

Heat injected in the water circuit

$$Q_{2,s} = q_{m,2,s}\, (h_{2,1,s} - h_{2,7,s})$$

The generator efficiency is the same of that in the cascade system, and the efficiency of Rankine cycle can be expressed as

$$\eta_{rankine,s} = (P_{turbine,s} - P_{pump,s}/\eta_{generator})/Q_{2,s}$$

4.2 Separate dish system

In the separate dish system, Stirling engines with the same number of dish collectors are directly put on the focuses of the dish collectors. Water is used for cooling the Stirling engines.

$T_{H,s}$ is chosen to be equal to outlet temperature of air in dish receiver. $T_{L,s}$ is chosen to be 310 K, the default expansion temperature in Fraser's dissertation [9] for the calculation of 4-95 NKII engine. k and γ are chosen the same value as that of the Stirling engines in the cascade system.

$$T_{R,s} = \frac{T_{H,s} - T_{L,s}}{\ln \dfrac{T_{H,s}}{T_{L,s}}}$$

$$e_s = \frac{T_{R,s} - T_{L,s}}{T_{H,s} - T_{L,s}}$$

$$\eta_{stirling,s} = \frac{T_{H,s} - T_{L,s}}{T_{H,s} + \dfrac{1 - e_s}{k - 1} \cdot \dfrac{T_{H,s} - T_{L,s}}{\ln \gamma}}$$

The power of Stirling engine

$$P_{stirling,s} = n_{dC} A_{dC} I_{DNI} \eta_{dC} \eta_{stirling,s}$$

5 Results and Conclusion

The results presented in Table 4 are issued using parameters in Table 1. Different results between two flow types of Stirling engine array are listed in Table 5.

Table 4: Some important results using typical parameters

Parameters	Value
η_{system}	0.1974
$\eta_{system,s}$	0.1962
$\eta_{stirling}$	0.3395
$\eta_{stirling,s}$	0.3786
$\eta_{rankine}$	0.2660
$\eta_{rankine,s}$	0.2678
$P_{generator}$	6×10^6 W
$P_{generator,s}$	5.826×10^6 W
$P_{stirling}$	3.552×10^5 W
$P_{stirling,s}$	4.909×10^5 W

Table 5: Results of Stirling engine array with two different flow types

x	Parallel flow				Counter flow			
	$T_{1,i}$ K	$T_{2,i}$ K	$P_{stirling}$ W	$\eta_{stirling}$ -	$T_{1,i}$ K	$T_{2,i}$ K	$P_{stirling}$ W	$\eta_{stirling}$ -
1	1073.15	327.17	5000	0.3648	1073.15	348.09	4867	0.3601
2	1022.38	329.80	4630	0.3599	1023.25	345.48	4541	0.3562
3	974.35	332.29	4280	0.3544	975.82	343.00	4230	0.3520
4	928.90	334.65	3949	0.3485	930.75	340.65	3934	0.3474
5	885.91	336.88	3635	0.3419	887.94	338.42	3654	0.3424
6	845.26	339.00	3338	0.3347	847.28	336.29	3387	0.3370
7	806.82	341.00	3057	0.3269	808.69	334.28	3134	0.3312
8	770.49	342.91	2792	0.3184	772.06	332.37	2894	0.3248
9	736.16	344.71	2541	0.3090	737.31	330.55	2666	0.3180
10	703.75	346.43	2304	0.2989	704.37	328.82	2450	0.3106

Nomenclature

A_{dC}	Aperture area of each dish collector, m^2
$A_{stirling,1}$	Heat transfer area of Stirling engine at air side, m^2
$A_{stirling,2}$	Heat transfer area of Stirling engine at water side, m^2
A_{tC}	Aperture area of each trough collector, m^2
d_{ap}	Aperture diameter of volumetric receiver, m
d_{cav}	Diameter of volumetric receiver cavity, m
$d_{i,air}$	Inner diameter of air tube, m
I_{DNI}	Direct Normal Irradiance, W/m^2
K	Incidence angle modifier of trough collector
$k_{stirling}$	Specific heat ratio of the working gas in Stirling engine
l_{cav}	Depth of volumetric receiver cavity, m
n	Amount of working gas in each Stirling engine, mol
n_2	Number of rows of the Stirling engine array
n_{se}	Speed of Stirling engine, s^{-1}
$n_{stirlingEngine}$	Number of Stirling engines in the Stirling engine array
p_c	Exhaust pressure of turbine, Pa
p_s	Main steam pressure of turbine, Pa
p_{amb}	Ambient pressure, Pa
p_{cp}	Water pressure after condensate pump, Pa
$p_{deaerator}$	Outlet pressure of deaerator, Pa
p_{dish}	Air pressure in dish, Pa
$P_{generator}$	Power of generator, W
p_{trough}	Air pressure in trough, Pa
q''	Heat flux, W/m^2
$q_{cond,tot}$	Total conduction loss
$q_{conv,tot}$	Total convection loss
$q_{dish,air}$	Energy absorbed by air in the dish collector

q_{in}	Solar energy launched into dish receiver aperture, W
$q_{m,1,r}$	Mass flow rate of air in each row of Stirling engine array, kg/s
$q_{m,2,r}$	Mass flow rate of water in each row of Stirling engine array, kg/s
$q_{rad,emit}$	Radiation emitted by dish receiver
$q_{rad,reflect}$	Reflected radiation by volumetric receiver, W
T_s	Main steam temperature of turbine
$T_{1,afterstirling}$	Air temperature after heating Stirling engine
T_{amb}	Ambient temperature, K
$T_{dish,inlet}$	Dish inlet temperature, K
$T_{dish,outlet}$	Dish outlet temperature
$T_{s,d}$	Designed mean steam temperature of turbine
$T_{trough,outlet}$	Trough outlet temperature
U	Overall heat transfer coefficient, W/(m^2·K)
$U_{stirling,1}$	Overall heat transfer coefficient of Stirling engine at air side, W/(m^2·K)
$U_{stirling,2}$	Overall heat transfer coefficient of Stirling engine at water side, W/(m^2·K)
v_{wind}	Ambient wind speed, m/s
x	Dryness fraction

Abbreviations

EES	Engineering Equation Solver
SAM	System Advisor Model
SES	Stirling Energy System

Greek Symbols

α_{eff}	Effective absorptance
δ_a	Thickness of air tube in volumetric receiver, m
δ_{ins}	Thickness of receiver insulating layer, m
$\Delta T_{oil,water,min}$	Minimum temperature difference between oil and water in the oil-to-water heat exchanger, K

ϵ_{insu}	Emissivity of reciver insulating layer
$\eta_{opt,0}$	Optical efficiency with an incidence angle of 0
$\eta_{shading}$	Shading factor
γ	Intercept factor
$\gamma_{stirling}$	Compression ratio of Stirling engine
λ_{insu}	Thermal conductivity of receiver insulating layer, W/(m·K)
ρ	Reflectivity
θ_{dish}	Dish aperture angle (0° is horizental, 90° is vertically down)

Subscripts

x	Stirling engine in column x

References

[1] D.Y. Goswami. *Principles of Solar Engineering, Third Edition*. CRC Press, 2015.

[2] Giorgio Cau and Daniele Cocco. Comparison of medium-size concentrating solar power plants based on parabolic trough and linear Fresnel collectors. *Energy Procedia*, 45(0):101–110, 2014.

[3] G. Franchini, A. Perdichizzi, S. Ravelli, and G. Barigozzi. A comparative study between parabolic trough and solar tower technologies in Solar Rankine Cycle and Integrated Solar Combined Cycle plants. *Solar Energy*, 98(PC):302–314, 2013.

[4] Roberto Cipollone, Andrea Cinocca, and Angelo Gualtieri. A new conversion section for parabolic trough - Concentrated Solar Power (CSP-PT) plants. In *Energy Procedia*, volume 45, pages 61–70, 2014.

[5] Omar Behar, Abdallah Khellaf, Kamal Mohammedi, and Sabrina Ait-Kaci. A review of integrated solar combined cycle system (ISCCS) with a parabolic trough technology. *Renewable and Sustainable Energy Reviews*, 39(0):223–250, 2014.

[6] Sara Ghaem. Modeling and Analysis of Hybrid Solar-Dish Brayton Engine. *SolarPACES Conference*, 2012.

[7] F. Formosa and G. Despesse. Analytical model for Stirling cycle machine design. *Energy Conversion and Management*, 51(10):1855–1863, 2010.

[8] A.J. Juhasz. A mass computation model for lightweight brayton cycle regenerator heat exchangers. In *8th Annual International Energy Conversion Engineering Conference*, 2010.

[9] P.R. Fraser. *Stirling dish system performance prediction model*. Madison, 2008.

[10] Pablo Coronel and K. P. Sandeep. Heat transfer coefficient in helical heat exchangers under turbulent flow conditions. *International Journal of Food Engineering*, 4(1), 2008.

[11] R W Serth. *Process heat transfer principles and applications*. Elsevier Academic Press, Amsterdam; London, 2007.

[12] John A. Duffie and William A. Beckman. *Solar Engineering of Thermal Processes: Fourth Edition*. Wiley, 2013.

[13] R. E. Hogan. AEETES - a solar reflux receiver thermal performance numerical model. *Solar energy*, 52(2):167–178, 1994.

[14] S. W. Churchill and M. Bernstein. A correlating equation for forced convection from gases and liquids to a circular cylinder in crossflow. *Journal of Heat Transfer*, 99(2):300–306, 05 1977.

[15] Robert Y Ma. Wind effects on convective heat loss from a cavity receiver for a parabolic concentrating solar collector. *Sandia National Laboratory*, SAND92-7293(September), 1993.

[16] Shuang-Ying Wu, Lan Xiao, Yiding Cao, and You-Rong Li. Convection heat loss from cavity receiver in parabolic dish solar thermal power system: A review. *Solar Energy*, 84(8):1342 – 1355, 2010.

[17] U. Leibfried and J. Ortjohann. Convective heat loss from upward and downward-facing cavity solar receivers: Measurements and calculations. *Journal of Solar Energy Engineering*, 117(2):75–84, 05 1995.

[18] A.A. Koenig and M. Marvin. Convection heat loss sensitivity in open cavity solar receivers. Technical report, Department of Energy, USA, 1981.

[19] William B Stine and Richard B Diver. A compendium of solar dish/stirling technology. Technical report, DTIC Document, 1994.

[20] M Romero-Alvarez and E Zarza. Concentrating solar thermal power. *Efficiency and Renewable Energy*, 2007.

[21] A. Der Minassians. *Stirling Engines for Low-temperature Solar-thermal-electric Power Generation*. University of California, Berkeley, 2007.

[22] M. Cavazzuti. *Optimization Methods: From Theory to Design Scientific and Technological Aspects in Mechanics*. Springer Berlin Heidelberg, 2012.

[23] W.B. Stine and R.W. Harrigan. *Solar energy fundamentals and design: with computer applications*. A Wiley-Interscience publication. John Wiley & Sons, Incorporated, 1985.